Comparison of the Asian Monsoon between the mid-Holocene and the Last Glacial Maximum

Seong-Joong Kim[1], Thomas J. Crowley[2], Bang Yong Lee[1], Bong-Chool Suk[3]

[1]Korea Polar Research Institute, KORDI
Songdo Techno Park, Incheon 406-840, Korea

[2]Division of Earth and Ocean Sciences
Duke University, Durham, NC 27708, USA

[3]Korea Ocean Research & Development Institute
Ansan PO Box 29, Seoul 425-600, Korea

1. Introduction

During the mid-Holocene the summer insolation was about 7% (30 W m^{-2}) higher than present at 65°N, whereas it was reduced by 3.5% (15 W m^{-2}) at 65°S, while during the Last Glacial Maximum (LGM) the solar insolation is almost similar to that of present. This variation of the solar insolation is due to the variation in orbital parameters (eccentricity, obliquity, and precession), which are out of phase with present in the mid-Holocene and in phase in the LGM. Even though the energy from the sun in the LGM was almost the same as present, the atmospheric CO_2 concentration was lower and ice sheets were formed over North America and northern Europe. These glacial conditions led to the different climate condition (e.g., CLIMAP, 1981).

Climate model simulations and paleoclimatic data suggest that two mechanisms exert the dominant forcing on millennial-scale variations in monsoon strength. First, changes in the orbit of the Earth, predominantly in the precession of the equinoxes, control the amount of insolation reaching the Earth as a function of season, and hence the ability of the Tibetan Plateau to warm in the summer (Prell and Kutzbach 1987). Second, changes in glacial boundary conditions (ice sheet topography and albedo, sea surface temperature (SST), and atmospheric greenhouse-gas concentrations) have been considered to alter the way in which the monsoon can respond to astronomical forcing (Manabe and Broccoli 1985).

In this study, we compare the change in the Asian monsoon between the mid-Holocene and the LGM using results obtained by a relatively fine resolution numerical model.

2. Model description and experiments

The simulations were performed with the Community Climate Model version 3 (CCM3) atmospheric general circulation model at T170 truncation. The transform grid has 512 x 256 cells, with a typical grid size of about 75 km with 18 vertical levels. This has identical physics to CCM3.6.6, but the computational aspects of the model have been re-written to allow more reliable and efficient operation on massively parallel computers as illustrated in Duffy et al., [2003]. Important physical processes are described in detail by Kiehl et al. [1998]. The CCM3 includes a comprehensive model of land surface processes known as the NCAR Land Surface Model (LSM; Bonan, 1998).

Three experiments are analyzed. The modern climate simulation, referred to as MOD, is forced by climatologically-averaged monthly sea-surface temperatures (SSTs) and sea ice distributions provided by NCAR, a specified CO_2 concentration of 355 ppm, and present land mask and topography. The

mid-Holocene experiment, called HOL, has identical conditions to the MOD experiment except for the orbital parameters which set for 6k BP. The third experiment features glacial boundary conditions. Over ocean the SST and sea ice are prescribed using climatologically averaged monthly data prepared with the August and February reconstructions by the CLIMAP (1981). The glacial surface topography was modified following the Ice-4G reconstructions and the land mask is modified to account for the lower sea level (~120 m). The atmospheric CO_2 concentration is reduced to 200 ppm following ice core data. Vegetation and soil types are unchanged except over glaciated surfaces. Land points arising due to sea level reduction are assigned a medium soil type. Orbital parameters set to 20k BP.

3. Results

Fig. 1 shows simulated winds at 1000 hPa. In winter, winds blow from the continent to ocean in the MOD experiment. This is due to the high pressure system over Siberia, which drives strong northwest winds in eastern Asia and northeast winds in the Arabian Sea. In summer, the wind pattern becomes reversed, blowing from the ocean. The most distinctive landward wind is the strong southwest Somali jet blowing from the Arabian Sea to India and Bay of Bengal. This landward wind pattern is due to the development of low pressure system over the Tibetan Plateau. The strong southwest wind in the Arabian Sea transfers moisture to the adjacent lands and results in high precipitation over eastern India and Bay of Bengal as illustrated later.

In the mid-Holocene winter, the increase in the sea level pressure over the Tibetan Plateau leads to the enhancement of seaward winds. A large increase in the northeast wind in the Indian Ocean and the Arabia Sea is visible (Fig. 1c). In summer, the deeper surface low pressure inside the continent intensifies the landward winds, especially the southwest wind in the Arabian Sea. An increase

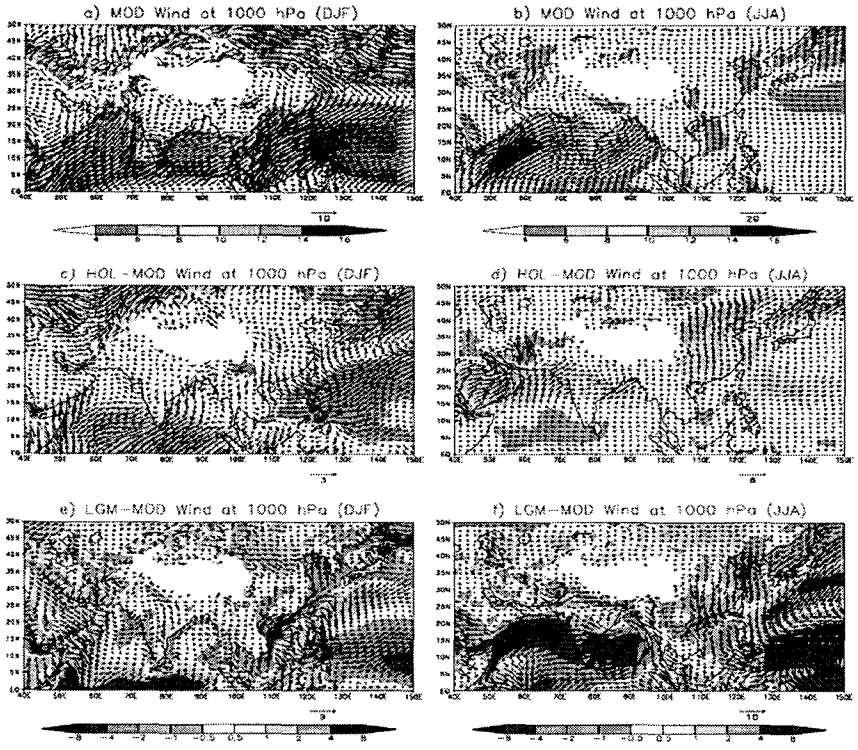

Fig. 1 Wind vectors at 1000 hPa for the MOD and the change.

in landward winds is also shown in the northeast Pacific. Overall, the mid-Holocene monsoon circulation appears to be substantially enhanced in both seasons.

In the LGM, the increase in surface pressure around the Tibetan Plateau tends to increase the anticyclonic circulation in winter. The northeast wind is enhanced in the Indian Ocean. However, the much larger increase in sea level pressure in the Middle East and Saudi Arabia leads to a more northerly component in the Arabian Sea than in MOD where the wind is north-easterly. In summer, the increase in sea level pressure over the northern Tibetan Plateau leads to marked decrease in southwest wind and thus, the summer monsoon circulation. Overall, in the LGM the monsoon circulation is enhanced in winter, whereas in summer the monsoon circulation, especially the southwest wind, is markedly weaker.

The spatial wind pattern is closely linked to the distribution of precipitation. Fig. 2 presents the simulated winter and summer precipitation in the MOD experiment and change from the HOL and LGM experiments. The high-resolution model appears to simulate precipitation reasonably well in comparison to observed precipitation (see Kim et al., 2006). For example, precipitation is low in northern and eastern China, Mongolia, and Saudi Arabia in winter as would be expected from the distribution of low-level winds. In summer, on the other hand, precipitation is large in most Asian regions. This is particularly the case in Bay of Bengal, India, and South Asia where precipitation is more than 8 mm per day. The high precipitation in those regions is due to the strong southwest wind in the Arabian Sea which transfers moisture to the adjacent lands.

In the mid-Holocene winter, there is little change in precipitation. This result is not surprising because there is no moisture source inside the continent. In

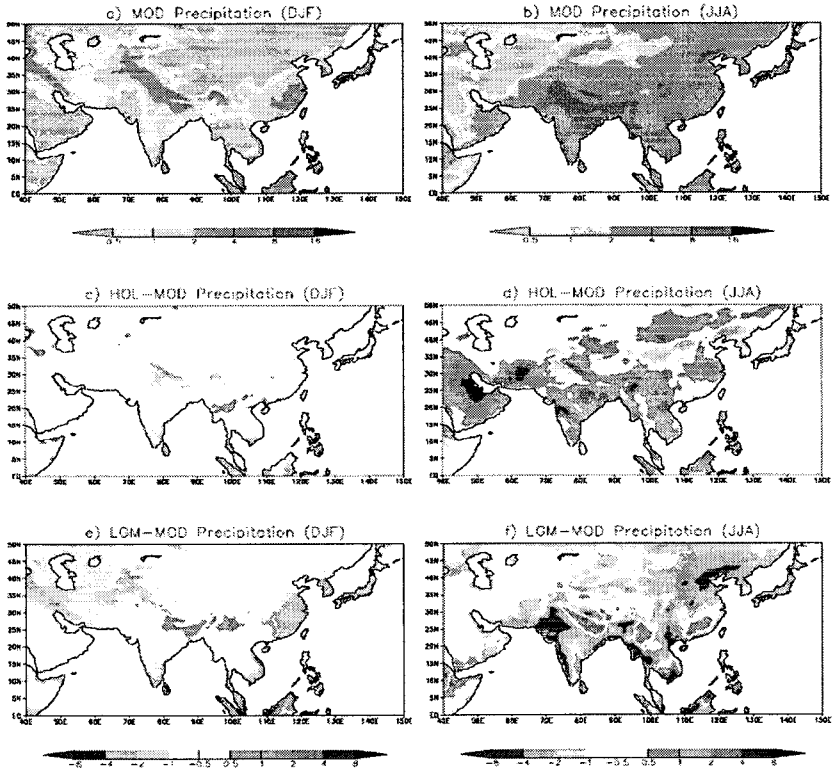

Fig. 2 Precipitation (mm/day) for the MOD and the change.

summer, on the other hand, precipitation is larger than MOD over most of Asia, especially over Saudi Arabia, India, South Asia, and north East Asia (Fig. 2d). This increase seems to be associated with the increase in landward winds. In the LGM winter, the change in precipitation is fairly small as in the case of HOL. In summer, precipitation decreases as well in most regions. The precipitation decrease is especially large in western India and western South Asia presumably due to the weakening of the southwest wind in the Indian Ocean.

4. conclusions

In conclusion, the Asian summer monsoon becomes stronger in the mid-Holocene and weaker in the LGM, while the winter monsoon increases in both periods. These model results agree with observational proxy evidence and other previous model simulations.

Acknowledgements This study was supported by the evolution of Asian monsoon of the Korea Ocean Research and Development Institute (PG05020) and projects of Studies on the Polar Atmosphere and Climate Change (PE06030) and paleoceanography and paleoclimate reconstruction for the future global warming (PE06010) of the Korea Polar Research Institute.

References

Bonan, G., 1998, The land surface climatology of the NCAR Land Surface Model coupled to the NCAR Community Climate Model. J. Clim., 11, 1307-1326.

CLIMAP, 1981, Seasonal reconstructions of the Earth's surface at the last glacial maximum. Geol Soc Amer Map Chart Ser, MC-36.

Duffy, P. B., B. Govindasamy, J. P. Iorio, J. Milovich, K. R. Sperber, K. E. Taylor, M. F. Wehner, and S. L. Thompson, 2003, High-resolution simulations of global climate, part 1: present climate. Clim. Dyn., 21, 371-390.

Kiehl, J. T., J. J. Hack, B. G. Bonan, B. A. Boville, D. L. Williamson, and P. Rasch, 1998, The National Center for Atmospheric Research Community Climate Model: CCM3. J. Clim., 11, 1131-1149.

Kim, S.-J., T. J. Crowley, D. J. Erickson, G. Bala, and P. B. Duffy, 2006, High-resolution climate simulation of the Last Glacial Maximum. Clim. Dyn., Submitted.

Manabe, S., and A. J. Broccoli, 1985, The influence of continental ice sheets on the climate of an ice age. J. Geophys. Res., 90, 2167-2190.

Prell, W. L., and J. E. Kutzbach, 1987, Monsoon variability over the past 150,000 years. J. Geophys. Res., 92, 8411-8425.